Indirect-Adaptive Sliding-Mode Voltage Control of the Switched-Inductor Z-Source Inverter

Mehran Jelodari Mamaghani [1]*, Mojtaba Hajihosseini [2] and Husam I. Shaheen [3]

***Abstract*— This research presents a new sliding-mode adaptive technique for stabilization of the output voltage of a single-phase Switched Inductor Z-source Inverter (SIZSI) as an interface in renewable energy sources. The proposed method is based on a sliding mode controller modified by an online adaptation of uncertain inverter parameters. The sliding mode controller improves the system's robustness in the face of external disturbances and preserves the system's output for any load, such as linear, nonlinear, and even changing loads. The proposed approach has been simulated in MATLAB/Simulink software package to show the controller's performance. The comparison results with the traditional sliding mode control have been conducted to validate the proposed method's superiority in resolving problems such as adaptive and robust against instantaneous deviations of input voltage and output current. The presented sliding-mode adaptive control technique shows a more efficient dynamic response to the system and less Total Harmonic Distortion (THD) than traditional controllers.**

***Index Terms*— Impedance source inverter, switched inductor Z-source inverter (SIZSI), voltage control, sliding mode control, indirect adaptive control.**

I. INTRODUCTION

THE importance of power quality has been rising due to the technological development in the Distributed Generation (DG). Renewable energy has different sources such as photovoltaic, biomass, wind, fuel cell, geothermal energy, combined heat and power, cooling, heat as well as power, and flow energy. When distributed generators, with their different types and technologies, are interconnected to the utility distribution system, some issues might arise [1], making it challenging to maintain high power quality. For this reason, power electronic converters, power conversion, and voltage control in power systems have increased significantly. Although DGs are complex systems, they have advantages like reducing the cost of energy and demand. DGs also increase reliability as uninterruptible and reserve power, reducing the distribution and transition network's loss, providing reactive power and power quality improvement, heat, and synchronal electricity generation. DGs are also beneficial for decreasing environmental pollution and greenhouse gases, such as CO2, and for fast response time and operation in the islanding network.

Due to the interconnection between different types and technologies of renewable energy sources, power electronics converters are necessary to convert the generated energy from renewable energy sources to DC power. DC power is transferred to the main power network after passing through different inverter and converter controllers based on DG type. The main challenge of DGs is the microgrids (MGs) operation with varying load characteristics and batteries in on-grid and islanding modes. DGs must be equipped with a controlled Voltage Source Converter (VSC) to overcome this challenge. Besides that, DGs need to satisfy the following conditions. According to IEEE-519 and IEC 62040-3 standards, the THD must be less than 5% for nonlinear loads. To meet these standards, the low-order harmonics must effectively be damped by a closed-loop controller from second to thirteenth frequencies. The controller should also properly regulate output voltages against input voltage and output current instantaneous deviations. As a result, a control system with the desired dynamical reaction is essential to update reference signals to reduce THD.

Impedance networks present an efficient means of power conversion between source and load in a wide range of power conversion applications. Different Z-source networks have proposed multiple methods and topologies. For example, adjustable drive speeds [2-3], uninterruptible power supply [4-5], distributed generation (fuel cell, photovoltaic (PV), wind, etc.) [6-7], battery or supercapacitor energy storage [8-9], electric vehicles [10-11], DC power distribution systems [12], the automatic pilot [13], flywheel energy storage systems [14], electronic loads [15], DC circuit breakers [16], etc. Multiple converter topologies with buck, boost, buck-boost, DC, AC, isolated, and non-isolated converters are accessible with the correct implementation of the impedance source network and various switching devices and topologies [17]. The initial impedance source network can be generalized as a network with two compound elements of linear energy storage consisting of capacitors and inductors. However, various network configurations may improve the circuit performance by adding various nonlinear elements to the impedance network, such as diodes, switches, or a mixture of both. The primary impedance source inverter has limitations in boost factor due to the constraint of low modulation index (M) and high duty ratio (D) [18]. In [17], the authors have proposed many topologies to

1- Mehran Jelodari Mamaghani is with Faculty of Electrical and Computer Engineering, Semnan University, Semnan, Iran.
2- Mojtaba Hajihosseini is with the Renewable Energy Systems, Faculty of Electrical Engineering and Computing, University of Zagreb, Croatia.
3- Husam I. Shaheen is with the Renewable Energy Systems, Faculty of Electrical Engineering and Computing, University of Zagreb, Croatia.
Corresponding author: mehranjelodari@semnan.ac.ir

tackle this limitation. One of these topologies, which is based on the impedance-source inverter, is the SIZSI. The problem of D and M conflict in the primary impedance source inverter has been solved using this topology [18].

Based on the classic ZSI (Z-source Inverter) impedance network inverter, a new topology known as the impedance network inverter with a switched inductor (SI) is presented in [18], which significantly increases the ability of voltage boost inversion. [19] presents a controller design method based on a power plant's nominal transformation function for a DG unit that operates in islanding mode. This method is suitable for an expected and balanced load but does not

cover large load oscillations. A statefeedback controller has been used to regulate the uninterruptible power supply (UPS) inverter in [20-22]. However, it suffers from slow response and lacks an asymmetrical method for dynamical stability. In [21], a control strategy is presented, which is replaced by a feedforward compensator component, decreasing load disturbance noticeably and simplifying the controller design. However, it is used only for balanced loads. In [23], a slide mode controller (SMC) has been designed to stabilize the output of a Quasi-Z-source converter. However, the SMC controller proposed in [23] faces the chattering phenomena which degrade the converter's output.

Regarding power electronic converters and their role in DGs to increase power quality and reliability of systems, we aim to improve the system reliability based on a combination of nonlinear control methods. Given the problems of switching and reducing output voltage in traditional inverters, which have caused limitations in the industry, individual abilities of impedance network inverters are used to mitigate the mentioned limitations. The proposed methods which work on SIZSI in the literature have focused mainly on changing and improving converter topologies, and voltage regulation is made mostly by PWM. Therefore, we present a new controller design method based on the adaptive sliding-mode approach for SIZSI. Compared with the conventional sliding-mode control, our proposed method regulates a converter in an extensive range by itself and has high output efficiency. Furthermore, the output power quality has been improved due to the controller's fast performance.

This paper is organized as follows: the second part describes the performance of the ZSI's fundamental control associated with the SIZSI. In the third part, the impedance network inverter via SI topology and voltage controller is explained by the indirect adaptive control method. In the fourth part, the simulation results are presented. The step-to-step scenario for SIZSI is based on the adaptive control method, and then a sliding mode control case has been given. The conventional single-phase inverter has been compared with the proposed new method with the existing sliding-mode methodology. In the end, the concluding remarks are presented.

I. Z-SOURCE IMPEDANCE NETWORK INVERTER

As shown in Fig. 1, the classical Z-source impedance network three-phase inverter topology consists of isolated inductors and capacitors linked in the X-form. Therefore, the switching operation introduced a shoot-through state for the upper and lower arms. With the rapid advancement of modern technologies, these forms can be seen. As a result, more applications of impedance network inverters are limited in some fields, which require high convertibility abilities, such as fuel cells, photovoltaic systems, and batteries.

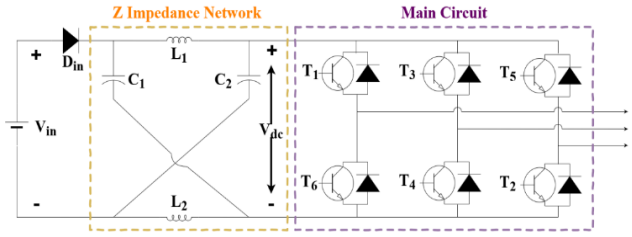

Fig. 1: Classic impedance network: the three-phase inverter topology.

In the past few years, advanced DC-DC conversion techniques such as Switched Capacitors (SC), Switched Inductors (SI), hybrid SC/SL, voltage multiplier cells, and voltage increase methods have frequently been studied. The objective is to reach a simple structure with high power density and efficiency. Therefore, integrating classic Z-source inverters and advanced DC/DC conversion promotion methods can be an excellent solution to improve the efficiency of Z-source inverters and their industrial applications [19].

A. Switched inductor Z-source inverter (SIZSI)

As mentioned earlier, SIZSI is proposed to tackle the limitations caused by the insubordinate voltage in the classical Z-source inverter wild voltage. The switched SI method has been combined with the classical Z-source inverter in this task. Therefore, a SIZSI is presented in this research. As shown in Fig. 2, the proposed inverter contains four inductors (L1, L2, L3, and L4), two capacitors (C1 and C2), and six diodes (D1, D2… D6). L1-L3, D1-D2-D3, and L2-L4, D4-D5-D6 perform high and low SL cell activities. Moreover, both SL cells store and transfer energy from capacitors to the DC bus under the main circuit's switching operations. The utilization principles in the primary circuit's switching states in the impedance network with SL are similar to the utilization principles of the classic impedance network. The single-phase SIZSI control schematic is shown in Fig. 2, which this paper proposes. In [18], the topology and operational principles are fully explained.

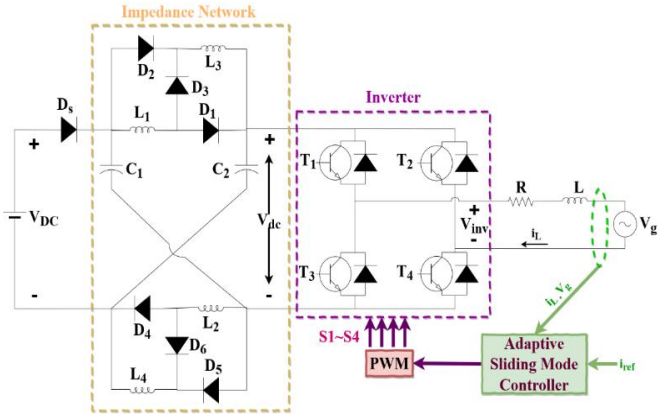

Fig. 2: The schematic of the Switched inductor Z-source with a single-phase inverter.

Energy is saved in the inductances of the impedance network by the dotted line in the yellow part when there is no resistance in the circuit. To obtain suitable efficiency in experimental circuits, It would be better than the saved energy returns to the source. In the impedance network with the dotted line in the yellow part, D_{in} sends back the imprisoned energy in the circuit to the source. The capacitors C_1 and C_2 save energy, then damp the current impulse waveform similar to L_1, L_2, L_3, L_4, which leads to damping voltage impulse waveform. In high-power applications, the current flow is achieved by diodes' parallel connection. Based on the voltage drop on each $D_2 - D_6$, the current is divided into diodes. The flowchart of the SIZSI with the adaptive sliding mode controller is shown in Fig.3. From this figure, it can be seen that the microgrid can work either in an islanded mode. In this case, the output power of the inverter is supplied directly to the load or in a grid-connected mode, where the output power is supplied to the primary grid.

II. The System Model and Control Strategy

A. The single-phase SIZSI dynamic model

To obtain the dynamic model of the system, Kirchhoff's Voltage Law (KVL) is given in Fig. 2. as follows:

$$V_R + V_L + V_g - V_{inv} = 0 \tag{1}$$

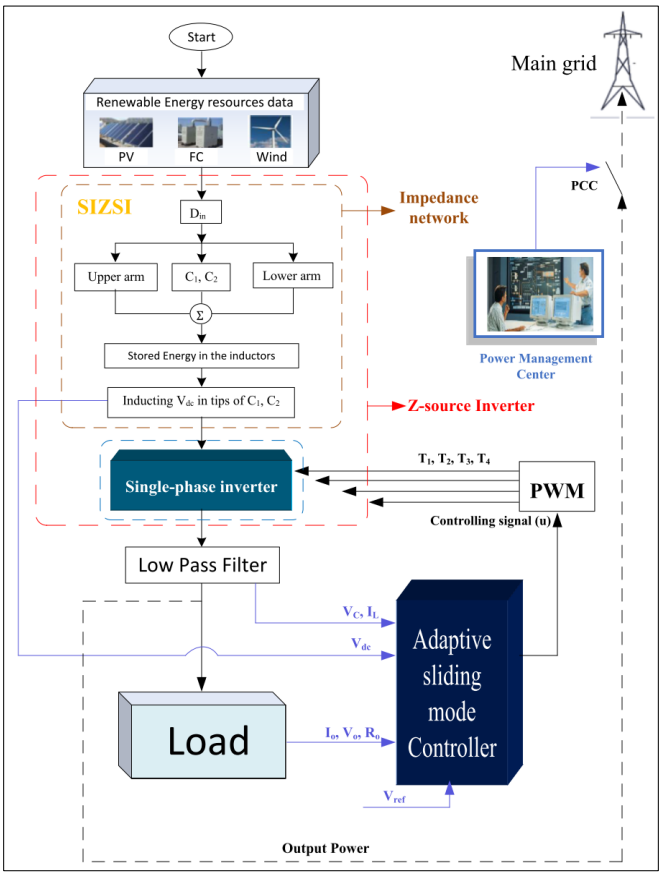

Fig. 3: SIZSI flowchart with the proposed adaptive sliding mode controller.

where V_R , V_L, V_g and V_{inv} are the resistor voltage, the inductor voltage, the grid voltage, and the inverter output voltage. So, regarding Fig.2, we have:

$$\begin{cases} V_L = L\dfrac{di_L}{dt} \\ V_R = R * i \\ V_{inv} = uV_{dc} \end{cases} \tag{2}$$

putting equations (2) into (1), we have:

$$\begin{aligned} & R + i_L + L\frac{di_L}{dt} + V_g \quad - uV_{dc} = 0 \\ & \rightarrow \frac{di_L}{dt} = \frac{1}{L}(-R * i_L - V_g + uV_{dc}) \end{aligned} \tag{3}$$

The inverter output current i_L is considered as the state variable, u the discrete input control signal, R, and L are transmission line resistors and inductors, respectively.

B. Designing the proposed controller

Eq. (4) is considered as the inverter dynamic in this section, which is linearized from Eq. (1). Here, R and V_{dc} are uncertain parameters of the system.

$$\dot{x} = -\frac{R}{L}x + \frac{V_{dc}}{L}u \tag{4}$$

It is assumed that x is measurable. However, an estimator has been used to facilitate the design of parameters matching rules for $\hat{R}$ and $\hat{V}_{dc}$. $\hat{R}$ and $\hat{V}_{dc}$ are estimation parameters of R and V_{dc}. It would be shown that $\hat{R} \rightarrow R$ and $\hat{V}_{dc} \rightarrow V_{dc}$. For this purpose, this estimation is considered:

$$\dot{\hat{x}} = -\frac{\hat{R}}{L}x + \frac{u}{L}\hat{V}_{dc} + K_a(x - \hat{x}) \tag{5}$$

where K_a is the observer gain and $\hat{x}$ is the x estimator, so we have:

$$\begin{cases} \tilde{x} = x - \hat{x} \rightarrow \hat{x} = x - \tilde{x} \\ \tilde{R} = R - \hat{R} \rightarrow \hat{R} = R - \tilde{R} \\ \tilde{V}_{dc} = V_{dc} - \hat{V}_{dc} \rightarrow \hat{V}_{dc} = V_{dc} - \tilde{V}_{dc} \end{cases} \tag{6}$$

By putting (6) into (5), we have:

$$\begin{aligned} & \frac{d}{dt}(x - \tilde{x}) = -\frac{(R - \tilde{R})}{L}(x - \tilde{x}) + \frac{u}{L}(V_{dc} - \\ & \tilde{V}_{dc}) + K_a\tilde{x} \rightarrow -\dot{\tilde{x}} = -\frac{R}{L}x + \frac{R}{L}\tilde{x} + \frac{\tilde{R}}{L}x - \frac{\tilde{R}}{L}\tilde{x} + \\ & \frac{u}{L}V_{dc} - \frac{u}{L}\tilde{V}_{dc} + K_a\tilde{x} - \dot{x} \rightarrow \dot{\tilde{x}} = \frac{R}{L}x - \frac{R}{L}\tilde{x} - \frac{\tilde{R}}{L}x + \\ & \frac{\tilde{R}}{L}\tilde{x} - \frac{u}{L}V_{dc} + \frac{u}{L}\tilde{V}_{dc} - K_a\tilde{x} + \dot{x} \end{aligned} \tag{7}$$

By putting (4) into (6), we have:

$$\begin{aligned} & \dot{\tilde{x}} = \frac{R}{L}x - \frac{R}{L}\tilde{x} - \frac{\tilde{R}}{L}x + \frac{\tilde{R}}{L}\tilde{x} - \frac{u}{L}V_{dc} + \frac{u}{L}\tilde{V}_{dc} - \\ & K_a\tilde{x} \pm \frac{R}{L}x + \frac{V_{dc}}{L}u \\ & \rightarrow \dot{\tilde{x}} = -\frac{\tilde{R}}{L}x + \frac{u}{L}\tilde{V}_{dc} - K_a\tilde{x} \end{aligned} \tag{8}$$

The following Lyapunov function is studied to create the adaption law:

$$V = \frac{1}{2}L\tilde{x}^2 + \frac{1}{2\gamma_1}\tilde{R}^2 + \frac{1}{2\gamma_2}\tilde{V}_{dc}^2 \quad (9)$$

where $\gamma_1 > 0$ and $\gamma_2 > 0$. The time derivative of the Lyapunov function needs to be negative to meet stability. Thus:

$$\dot{V} = L\dot{\tilde{x}}\tilde{x} + \frac{1}{\gamma_1}\dot{\tilde{R}}\tilde{R} + \frac{1}{\gamma_2}\dot{\tilde{V}}_{dc}\tilde{V}_{dc} < 0 \quad (10)$$

By putting (8) into (10), we have:

$$\begin{aligned} \dot{V} = {} & \tilde{x}\left(-\tilde{R}x + uV_{dc} - K_aL\tilde{x}\right) + \frac{1}{\gamma_1}\dot{\tilde{R}}\tilde{R} \\ & + \frac{1}{\gamma_2}\dot{\tilde{V}}_{dc}\tilde{V}_{dc} \\ \rightarrow \dot{V} = {} & K_aL\tilde{x}^2 + \left(-\tilde{R}x\tilde{x} + uV_{dc}\tilde{x}\right) + \frac{1}{\gamma_1}\dot{\tilde{R}}\tilde{R} \\ & + \frac{1}{\gamma_2}\dot{\tilde{V}}_{dc}\tilde{V}_{dc} \\ \rightarrow \dot{V} = {} & K_aL\tilde{x}^2 + \left(-x\tilde{x} + \frac{1}{\gamma_1}\dot{\tilde{R}}\right)\tilde{R} + (\tilde{x} \\ & + \frac{1}{\gamma_2}\dot{\tilde{V}}_{dc})\tilde{V}_{dc} \end{aligned} \quad (11)$$

To eliminate the parameters in parentheses:

$$\begin{aligned} & -x\tilde{x} + \frac{1}{\gamma_1}\dot{\tilde{R}} = 0 \rightarrow \dot{\tilde{R}} = \gamma_1 x\tilde{x} \\ & \tilde{x} + \frac{1}{\gamma_2}\dot{\tilde{V}}_{dc} = 0 \rightarrow \dot{\tilde{V}}_{dc} = \gamma_2\tilde{x} \end{aligned} \quad (12)$$

To define the sliding-mode control law, the switching surface is defined as follows:

$$\begin{aligned} & S = \tilde{x} \rightarrow \dot{S} = \dot{\tilde{x}} = 0 \rightarrow -\frac{\tilde{R}}{L}x + \frac{u}{L}\tilde{V}_{dc} - K_a\tilde{x} = \\ & 0 \rightarrow u_{eq} = \frac{L}{\tilde{V}_{dc}}(K_a\tilde{x} + \frac{\tilde{R}}{L}x) \end{aligned} \quad (13)$$

Finally, the control signal would be defined as:

$$u = \rightarrow u_{eq} - K_s sign(S) \quad (14)$$

III. The Simulation Results

At first, the performance of the SIZSI is examined by applying the proposed controller under ohmic, ohmic-inductive, and nonlinear load in sections 4-1. The controller and system parameters are described in Table I.

TABLE I
Controller and System Parameters.

Parameter	Introduction						Value
F	Switching frequency						15000Hz
V_{DC}	DC voltage input						110V
ω_r	Voltage angular frequency						314.16
L	Filter inductive						22 mH
C	Filter capacitor						250 µF
L_1, L_2, L_3, L_4	Inductance of SIZSI						1mH
C_1, C_2	Capacitor in SIZSI						300µF
D_{in}, D_2…D_6	Diode in SIZSI						
	V_f	R_{on}	R_s				C_s
	0.8	0.001	500				250 nF
T_1, T_2, T_3, T_4	Thyristor in inverter						
	R_{on}		R_s				C_s
	1×10^{-3}		100000				inf
MOSFET $_{1,\ldots6}$	MOSFET in MB method						
	R_{on}	R_d	R_s	L_{on}	I_c	V_f	Cs
	0.1Ω	0.01 Ω	1×10^{-5}	0	0	0	inf
λ	Control parameters						15000
Kv							0.8
Ks							0.9

A. The controlling scenario for SIZSI based on indirect adaptive control

Six steps consider a scenario for showing the controller's performance under different load characteristics. In this scenario, no load is connected to the inverter output from the simulation time to 0.1 seconds (the first step). From seconds 0.1 to 0.3, the first ohmic load enters the circuit (the second step). From 0.3 to 0.5, the second ohmic load is added (the third step). The ohmic-inductive load is added from 0.5 to 0.7 seconds (the fourth step). At 0.7, the loads leave the circuit (the fifth step). At 0.8 seconds, the nonlinear load connects to the circuit and remains in the circuit for 1s, which is the end of the simulation (the sixth step). Table II shows the steps and the scenario of the simulation by SIZSI.

Fig. 4 shows the proposed control method's load and reference voltage waveform. In the zoom-out case of Fig. 4, the output signal of the inverter follows the reference signal, while it has a fast and suitable reaction just 0.006 s after the beginning of the simulation. This shows the fast response of the proposed controller to the system. Fig. 4 (a) shows that the output voltage of the inverter has a constant amount throughout the simulation, which, despite load variations, indicates that the controller is robust and adaptive to load variations. Compared to the input DC source shows no decrease, which reflects the advantage of

the impedance network inverter/ SIZSI over the traditional inverters.

TABLE II
Scenario of the Simulation by the Proposed Controller

	Time of Simulation						
	$0 \le t < 0.1s$	$0.1 \le t < 0.3s$	$0.3 \le t < 0.5s$	$0.5 \le t < 0.7s$	$t = 0.7s$	$0.7 \le t < 0.8s$	$0.8 \le t \le 1s$
Loads							
No Load	First step	———	———	———	Fifth step		———
First Ohmic Load :100 Ω		Second step	———	———			———
Second Ohmic Load: 20 Ω		———	Third step	———			———
Ohmic-Reactance Load: 10 Ω + 5 m H		———	———	Forth step			———
Dischargin g all of loads		———	———	———			———
None – Linear Load: 18Ω + 8200 μF		———	———	———			Sixth step

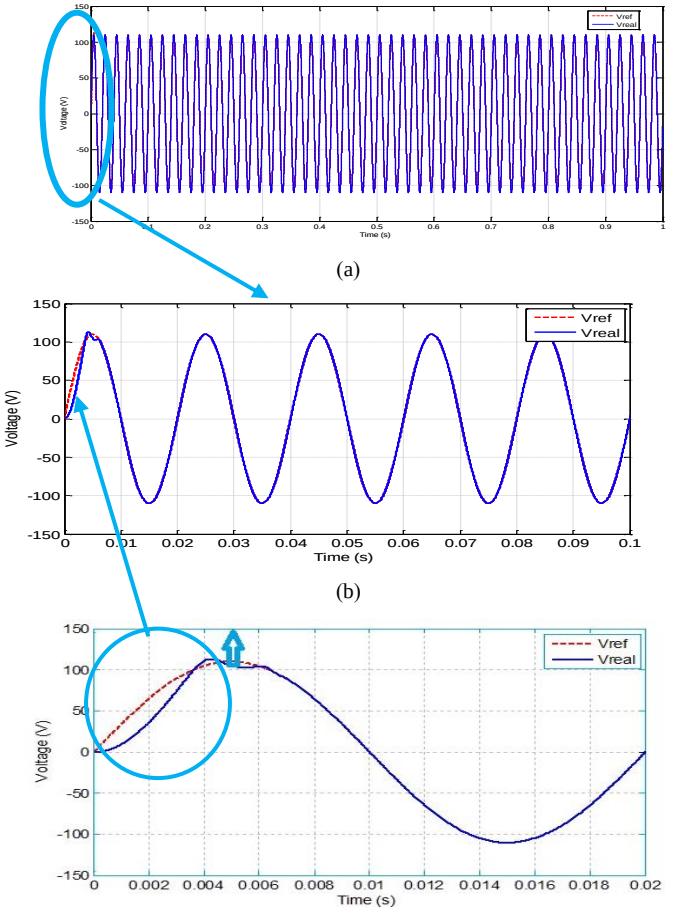

Fig. 4. Load and reference voltage waveforms by the proposed control method. (a) From the start to the end of the simulation. (b) From the beginning of the simulation to 0.1s. (c) From the start of the simulation to 0.02s

According to Figs. 5, 6, and 7, there is not any instability in the waveform of the output current. However, the two ohmic loads and an inductance load create disturbance in the system which means a suitable adaptation, high strength, and controlling fast response in an extensive range of disturbance and load changing. In these Figs. The inductive load adds in the second to fifth steps progressively. Figs. 9, 10, and 11 are the repeated cases of Figs. 5, 6, and 7, which compare the load current waveforms with the load voltage waveforms. Due to the existing inductance, the domain of currents is shorter than voltages.

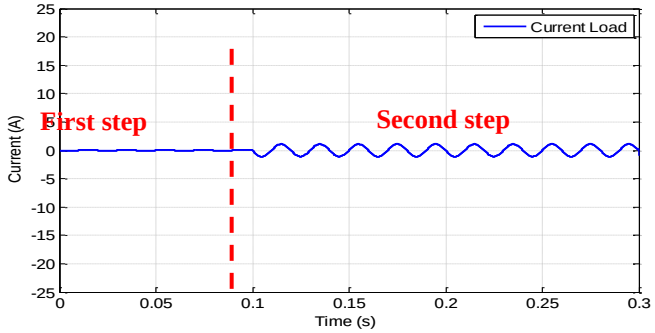

Fig. 5. Load the current waveform in the second step of the scenario.

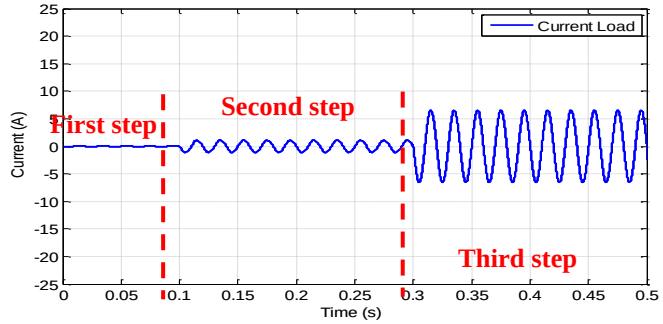

Fig. 6 Load the current waveform in the third step of the scenario.

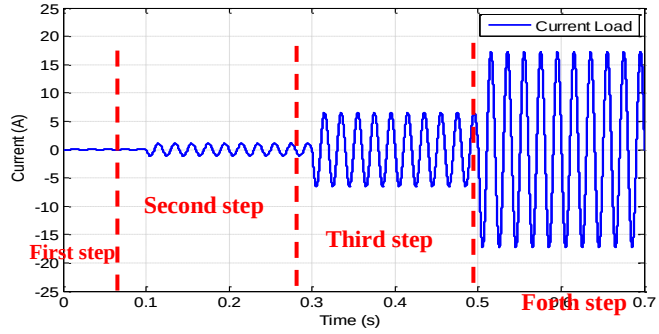

Fig. 7. Load the current waveform in the fourth step of the scenario

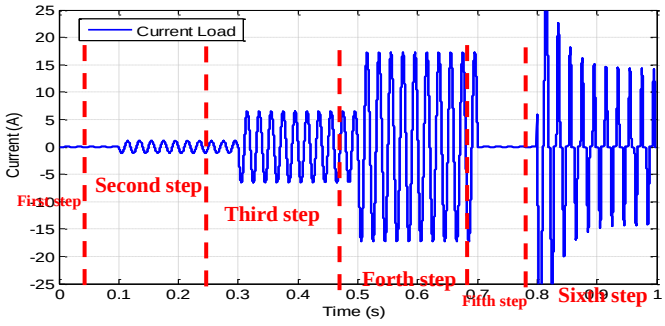

Fig. 8. Load current waveform in the fifth and sixth steps of the scenario.

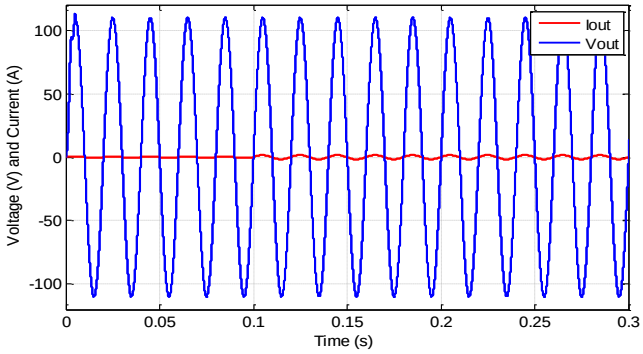

Fig. 9. Load current and voltage waveform in the second step of the scenario.

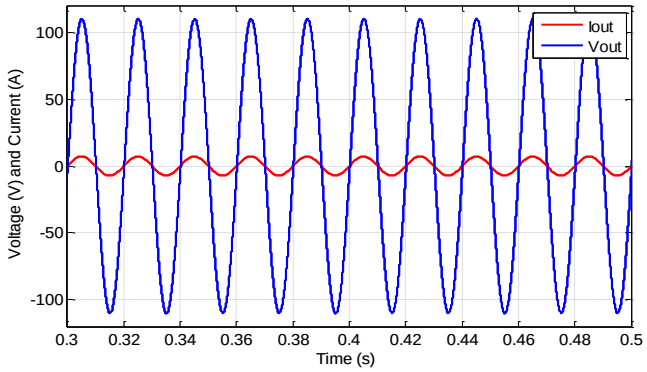

Fig. 10. Load current and voltage waveform in the third step of the scenario

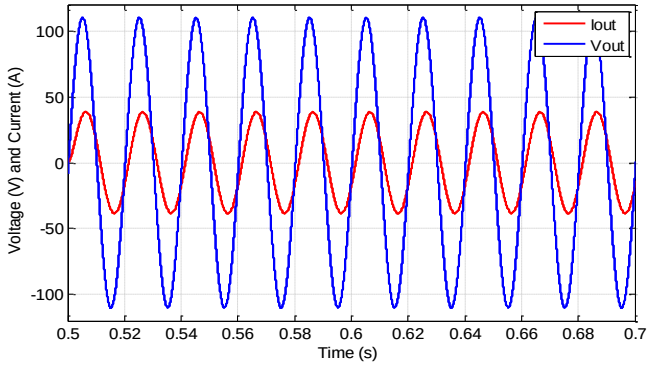

Fig. 11. Load current and voltage waveform in the fourth step of the scenario.

Figs. 8 and 12 show the result of the study on a nonlinear load in the sixth step. This nonlinear load has been simulated according to the IEEE standard. According to this, the controller presents a fast and acceptable response. The output voltage signal, which has been simulated, is in the time field. If we want to see signals caused by nonlinear load harmonics in a frequency field, we need to use the FFT (Fast Fourier Transform). It presents signal offsets in the frequency field. Here, the horizontal axes of the 13 show the frequency, and the vertical axes show the frequency domain value based on the output voltage signal. You can find the value of the frequency domain in 50 Hz.

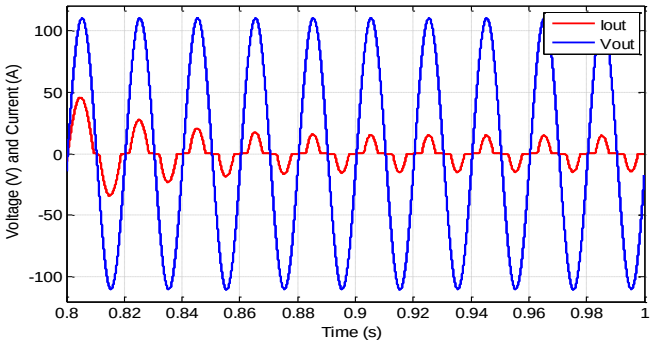

Fig. 12. Load current and voltage waveform in the fifth and sixth steps of the scenario.

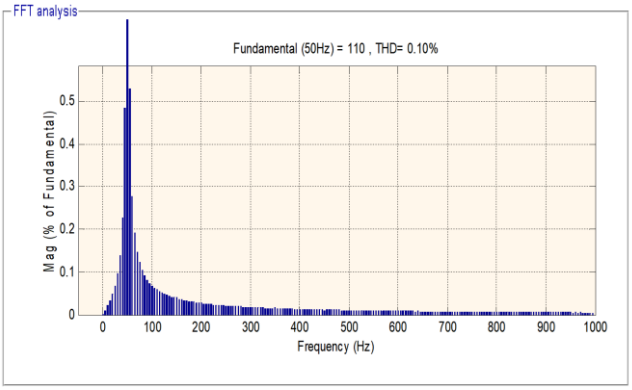

Fig. 13. Harmonic spectrum waveform based on SIZSI.

B. The sliding-mode control on traditional single-phase inverter

Finally, Fig. 14 shows the comparison between the proposed controller and conventional inverter. The load has been connected to both systems. The load properties are mentioned in Table II.

In the first step, by connecting load, the proposed method voltage output has a sinusoidal wave. However, the conventional method of output voltage has distortion (Fig. 14.a). The output voltage is almost identical when Ohmic load is applied to both systems. Fig. 14. c and d show ohmic losses. In Fig. 14. e fourth step, both outputs are the same. In fig. 14. f, the difference between the proposed and conventional methods can be seen. The first pick on of the conventional method has some harmonics compared to the proposed method. These figures show that the proposed method is more robust to changes. When a change in load happens, the proposed method can maintain better voltage output.

In Fig. 14. g the output voltage for nonlinear load displays the main advantages of the proposed method. In nonlinear load, the conventional method performance is decreased. The suggested method voltage remains sinusoidal, but the conventional output has distortion.

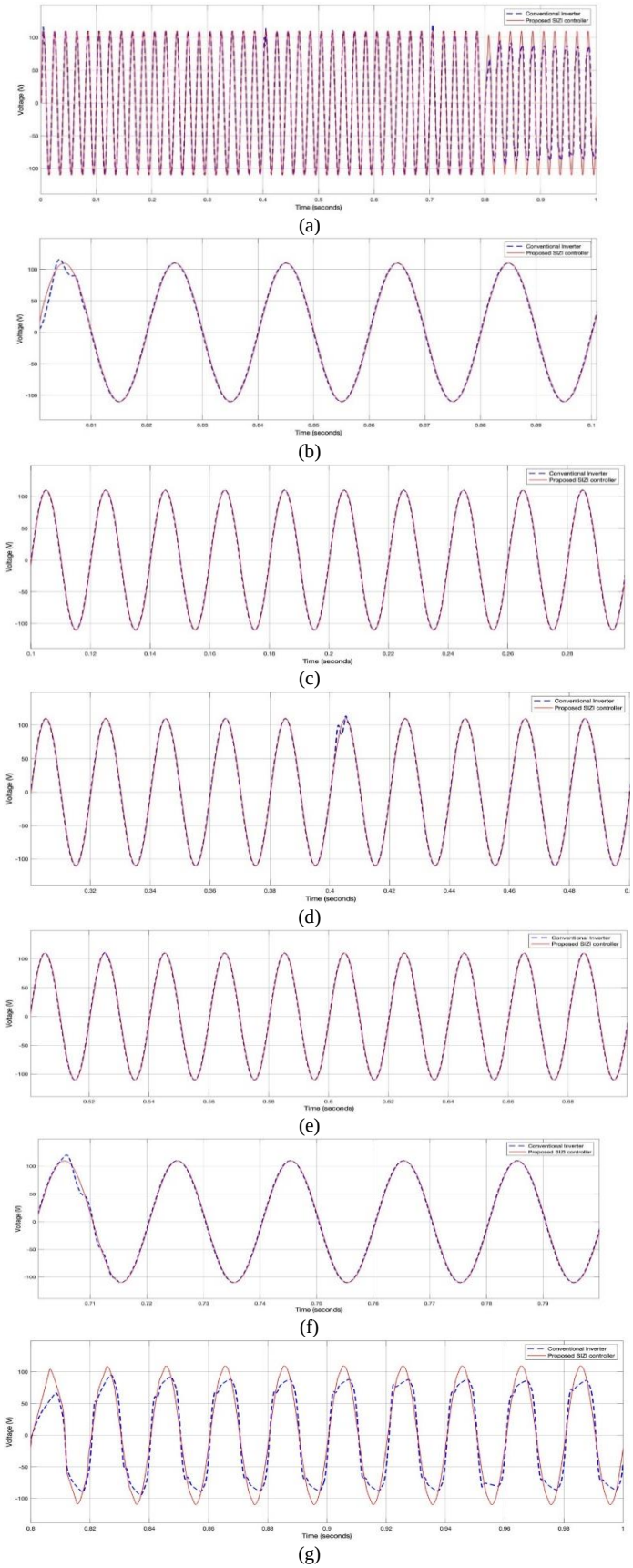

Fig. 14. Voltage comparison between the proposed controller and conventional inverter. (a) the voltage for all six steps, (b) first step(no load), (c) second step (first ohmic load), (d) third step (second ohmic load), (e) fourth step(ohmic and reactance load), (f) fifth step(discharging all load), and (g) six-step (nonlinear load).

IV. Conclusion

In this paper, the indirect adaptive controller was studied to control the inverter voltage of a switched impedance source with a SI or SIZSI under various load characteristics. The simulation results show that the controller is adaptive to load changes and follows the reference signal. It is resistant, has a fast and good reaction to load changes, and gives the generated inverter voltage to the reference voltage. Furthermore, it generates power with the desired quality that meets global standards. Due to the unique characteristics of the impedance network located between the input source and the main circuit of the inverter, the proposed inverter tackles the problems faced by traditional inverter limitations and by the classical Z-source inverter. Finally, to show the superiority of the proposed controller on SIZSI, a comparison was made on the traditional single-phase inverter by controlling voltage in the sliding-mode controller. This way, as seen in Fig. 14 (a, b), the voltage control has a faster and better dynamic response via indirect adaptive controller than the sliding-mode control. In Fig. 14, the comparison shows the advantages of the proposed method. In nonlinear load, the proposed method can deliver better quality voltage. Since realistic loads are nonlinear, this better performance is very desirable in renewable energy sources. The load in renewable energy sources can change a lot. The voltage output in the conventional system due to changes, as can be seen in Fig. 14, is more sensitive, which causes lower quality voltage output. However, the proposed method is more stable to load change. This stability is beneficial in systems with changes in load, such as renewable energy sources.

REFERENCES

[1] I. El-Samahy and E. El-Saadany, "The effect of DG on power quality in a deregulated environment," IEEE Power Engineering Society General Meeting, 2005, San Francisco, CA, 2005, pp. 2969-2976 Vol. 3, doi: 10.1109/PES.2005.1489228.

[2] F. Z. Peng, X. Yuan, X. Fang, and Z. Qian, "Z-source inverter for adjustable speed drives," *IEEE Trans. Power Electron.*, vol. 1, no. 2, pp. 33–35, Jun. 2003.

[3] R. Sankar and D. Sarala, "Design and implementation of improved Z-source inverter fed induction motor for wind applications," 2017 International Conference on Energy, Communication, Data Analytics and Soft Computing (ICECDS), Chennai, 2017, pp. 3665-3670, doi: 10.1109/ICECDS.2017.8390147.

[4] Z. J. Zhou, X. Zhang, P. Xu, and W. X. Shen, "Single-phase uninterruptible power supply based on Z-source inverter," *IEEE Trans. Ind. Electron.*, vol. 55, no. 8, pp. 2997–3004, Aug. 2008.

[5] K. Chitra and V. Kamatchikannan, "Performance Comparison of Three PWM Techniques for Three-Phase On-Line UPS with Switched Inductor Z-Source Inverter," 2018 International Conference on Circuits and Systems in Digital Enterprise Technology (ICCSDET), Kottayam, India, 2018, pp. 1-6, doi: 10.1109/ICCSDET.2018.8821187.

[6] A. Gautam, A. K. Sharma, A. Pareek, and R. Singh, "Analysis of Combined Z-Source Boost DC-DC Converter for Distributed Generation Systems," 2018 International Conference on Inventive Research in Computing Applications (ICIRCA), Coimbatore, 2018, pp. 1162-1167, doi: 10.1109/ICIRCA.2018.8597423.

[7] M. Jahanshahi Zeitouni, A. Parvaresh, S. Abrazeh, S.-R. Mohseni, M. Gheisarnejad, and M.-H. Khooban, "Digital twins-assisted design of next-generation advanced controllers for power systems and electronics: Wind turbine as a case study," Inventions, vol. 5, no. 2, p. 19, 2020.

[8] J. Liu, S. Jiang, D. Cao, and F. Z. Peng, "A digital current control of quasi-Z-source inverter with battery," *IEEE Trans. Ind. Informat.*, vol. 9,no. 2, pp. 928–936, May 2017.

[9] S. e. Boukebbous, D. Kerdoun, N. Benbaha, H. Ammar and A. Bouchakour, "Performance Enhancement of Grid-Off Photovoltaic Pumping System-Quasi Z Source Inverter by Hybrid Battery-Supercapacitor Energy Storage," 6th International Renewable and Sustainable Energy Conference (IRSEC), Rabat, Morocco, 2020, pp. 1-6, doi: 10.1109/IRSEC.2018.870289.

[10] M. Shen, A. Joseph, J.Wang, F. Z. Peng, and D. J. Adams, "Comparison of traditional inverters and Z-source inverter for fuel cell vehicles," IEEE Trans. Power Electron., vol. 22, no. 4, pp. 1453–1463, Jul. 2021.

[11] J. Srijeeth, V. C. Thiagarajan and S. R. Mohanrajan, "Z-Source Dual Active Bridge Bidirectional AC-DC Converter for Electric Vehicle Applications," 2018 IEEE International Conference on Power Electronics, Drives and Energy Systems (PEDES), Chennai, India, 2018, pp. 1-4, doi: 10.1109/PEDES.2018.8707465.

[12] Y. P. Siwakoti and G. Town, "Performance of distributed DC power system using quasi Z-source inverter based DC/DC converters," in Proc. Appl. Power Electron. Conf. Expo., Mar. 17–21, 2020, pp. 1946–1953.

[13] A. S. Khlebnikov and S. A. Kharitonov, "Application of the Z-source converter for aircraft power generation systems," in Proc. Int. Workshop Tuts. Electron Devices Mater., Jul. 2008, pp. 211–215.

[14] S. J. Amodeo, H. G. Chiacchiarini, and A. R. Olivia, "High-performance control of a DC/DC Z-source converter used for an excitation field driver," IEEE Trans. Power Electron., vol. 27, no. 6, pp. 2947–2957, Jun. 2012.

[15] J. C. R. Caro, F. Z. Peng, H. Cha, and C. Rogers, "Z-source-converter based energy-recycling zero-voltage electronic loads," IEEE Trans. Ind. Electron., vol. 56, no. 12, pp. 4894–4902, Dec. 2009.

[16] J. Shu, S. Wang, J. Ma, T. Liu and Z. He, "An Active Z-Source DC Circuit Breaker Combined With SCR and IGBT," in IEEE Transactions on Power Electronics, vol. 35, no. 10, pp. 10003-10007, Oct. 2020, doi:10.1109/TPEL.2020.2980543.

[17] Y. P. Siwakoti, F. Z. Peng, F. Blaabjerg, P. C. Loh, and G. E. Town, "Impedance-source networks for electric power conversion part I: A topological review," *IEEE Trans*. on power electronics, vol. 30, no. 2, pp. 699-716, 2014.

[18] M. Zhu, K. Yu, and F. L. Luo, "Switched inductor Z-source inverter," *IEEE Trans. Power Electron.*, vol. 25, no. 8, pp. 2150–2158, Aug. 2010.

[19] J. W. Jung and A. Keyhani, "Control of a fuel cell based Z-source converter," *IEEE Trans. Energy Convers*., vol. 22, no. 2, pp. 467–476, Jun. 2007.

[20] U. Borup, F. Blaabjerg, and P. Enjeti, "Sharing of nonlinear load in parallel-connected three-phase converters," *IEEE Trans*. Ind. Appl., vol. 37, no. 6, pp. 1817–1823, Nov./Dec. 2001.

[21] J. Guerrero, L. G. De Vicuña, J. Miret, J. Matas, and J. Cruz, "Output impedance performance for parallel operation of UPS inverters using wireless and average current-sharing controllers," in *2004 IEEE 35th Annual Power Electronics Specialists Conference (IEEE Cat. No. 04CH37551)*, 2004, vol. 4: IEEE, pp. 2482-2488.

[22] E. Coelho, P. Cortizo, and P. Garcia, "Small-signal stability for parallel connected inverters in stand-alone AC supply systems," *IEEE Trans.* Ind. Appl., vol. 38, no. 2, pp. 533–542, Mar./Apr. 2020.

[23] N. Saeed, A. Ibrar, and A. Saeed, "A review on industrial applications of Z-source inverter," *Journal of Power and Energy Engineering*, vol. 5, no. 9, pp. 14-31, 2017.